



# Identification of Novel Genes and Associated Drugs in Advanced Clear Cell Renal Cell Carcinoma by Bioinformatic Methods

Meiqi Lu,<sup>1</sup> Liangxiang Xiao,<sup>1</sup> Bo Xu<sup>1</sup> and Qing Gao<sup>1,2</sup>

<sup>1</sup>Department of Nephrology, Zhongshan Hospital of Xiamen University, School of Medicine, Xiamen University, Xiamen, China

<sup>2</sup>The Third Clinical Medical College, Fujian Medical University, Fuzhou, China

The current work screened differentially expressed genes (DEGs) related to advanced clear cell renal cell carcinoma (ccRCC) and found potential biomarkers and drugs for advanced ccRCC. After analyzing GSE53757 and GSE66271, we identified DEGs and performed the functional annotation, pathway enrichment, validation, survival analysis, and candidate drug analysis. We obtained 861 common DEGs from datasets between advanced ccRCC tissues and normal kidney tissues. Besides, we performed functional analysis under ontological conditions and carried out pathway analysis. The five most stable core gene groups and top 10 genes were screened using the Cytoscape software. We performed functional and pathway analyses again and found that the core genes were similar to total DEGs. After verification, the expression trends of the 10 hub genes did not change. Survival analysis showed high expressions of *TOP2A*, *BIRC5*, *BUB1*, *MELK*, *RRM2*, and *TPX2* genes, suggesting that they might participate in cancer occurrence, migration, and relapse of ccRCC. The gene-drug analysis showed that gallium nitrate, cladribine, and amonafide were strongly associated with *RRM2* and *TOP2A*. We found that *RRM2* and *TOP2A* might be predictive biomarkers and novel targeted therapy for advanced ccRCC. These drugs (gallium nitrate, cladribine, and amonafide) might be used for treating advanced ccRCC.

**Keywords:** amonafide; bioinformatics; cladribine; clear cell renal cell carcinoma; gallium nitrate

Tohoku J. Exp. Med., 2022 October, 258 (2), 79-90.

doi: 10.1620/tjem.2022.J059

## Introduction

Kidney cancer comprises around 3% of overall cancer cases, and its morbidity has increased by 2% annually worldwide for the past 20 years (Ferlay et al. 2018). Renal cell carcinoma (RCC) refers to a normal renal parenchymal lesion and is responsible for approximately 90% of all kidney cancer cases. Clear cell renal cell carcinoma (ccRCC) is a primary renal cell carcinoma subtype comprising approximately 80% of all RCC. Compared to other cancer subtypes, ccRCC has higher tumor recurrence and metastasis rates (Dong et al. 2019; Ljungberg et al. 2019). Since ccRCC does not have sensitivity to radiotherapy, chemotherapy, and immunotherapy, surgery is the primary treatment (Zhang et al. 2021). In the last decade, several studies identified diagnostic markers for ccRCC. However, as the mechanism of molecular regulation is not clear, effective drugs have not been administered clinically. Thus, it is nec-

essary to detect biomarkers and drugs to treat ccRCC.

The Gene Expression Omnibus (GEO) database functions as a comprehensive database for collecting tumor-related data. It contains sequencing results from all over the world. Recent studies have mined biomarkers of lung cancer (Long et al. 2020), breast cancer (Li et al. 2018), gastric cancer (Cao et al. 2018), pancreatic cancer (Ren et al. 2021) as well as other tumors through bioinformatics analysis of the GEO database. These biomarkers might contribute to diagnosing and treating diseases. In the current work, we searched for advanced ccRCC along with matched non-carcinoma renal tissues using the GEO database. We then mined differentially expressed genes (DEGs) for Gene Ontology (GO) enrichment, Kyoto Encyclopedia of Genes and Genomes (KEGG) pathway enrichment, gene-drug analysis, and protein-protein interaction (PPI) analysis for identifying possible biomarkers and therapeutic agents for advanced ccRCC.

Received June 18, 2022; revised and accepted July 13, 2022; J-STAGE Advance online publication July 28, 2022

Correspondence: Qing Gao, Department of Nephrology, Zhongshan Hospital Affiliated to Xiamen University, No. 201-209 Hubinnan Road, Siming District, Xiamen 361000, China.

e-mail: qinggao\_neph1@163.com

©2022 Tohoku University Medical Press. This is an open-access article distributed under the terms of the Creative Commons Attribution-NonCommercial-NoDerivatives 4.0 International License (CC-BY-NC-ND 4.0). Anyone may download, reuse, copy, reprint, or distribute the article without modifications or adaptations for non-profit purposes if they cite the original authors and source properly.

<https://creativecommons.org/licenses/by-nc-nd/4.0/>

## Materials and Methods

### Data

GEO is a publicly available oncogenomic database, and accessing it does not require ethics committee approval (Barrett et al. 2013). We obtained the advanced ccRCC datasets GSE53757 and GSE66271 from the GEO database (<https://www.ncbi.nlm.nih.gov/geo/>). GPL570 (Affymetrix Human Genome U133 Plus 2.0 Array) was used as a platform for microarray datasets. The GSE53757 dataset has 60 advanced ccRCC samples and 60 healthy renal samples, while the GSE66271 dataset has 12 advanced ccRCC samples and 13 healthy renal samples (Table 1).

### Screening for DEGs

The DEGs in advanced ccRCC were compared to normal tissues from the GSE53757 and GSE66271 datasets and analyzed by adopting the GE02R online tool (<https://www.ncbi.nlm.nih.gov/geo/geo2r/>).  $P < 0.05$  and  $|\log FC| > 2$  were regarded to be statistically significant. A log FC value  $> 2$  indicated that the genes were upregulated, whereas a log FC value  $< -2$  indicated that the genes were downregulated. The DEGs were shown using the Hiplot online drawing website (<https://hiplot.com.cn/>). We identified the genes that were common to the GSE53757 and GSE66271 datasets. The Venn diagram was used to visualize the intersecting genes (<http://bioinformatics.psb.ugent.be/webtools/Venn/>) (Jia et al. 2021).

### Functional annotations for DEGs

We imported the selected DEGs into the Database for Annotation, Visualization, and Integrated Discovery (DAVID) (<https://david.ncifcrf.gov/>) (Dennis et al. 2003), which is an online database for GO as well as the KEGG pathway enrichment for DEGs, with the threshold of  $P < 0.05$ .

### Establishing the protein-protein interaction (PPI) network

We constructed the PPI network on the basis of the STRING online database (<https://string-db.org/>) (Szklarczyk et al. 2021), and the Cytoscape software (<http://www.cytoscape.org/>) was adopted for visualization. Based on the cytoHubba plug-in, we selected the top 10 hub genes from the PPI network. Modules with the highest significance throughout the PPI network were constructed with the MCODE plug-in. We visualized the intersection of the top 10 genes and the five most stable core genes with a Venn diagram.

### Functional enrichment analyses of the core genes

To conduct GO and KEGG pathway enrichment, we uploaded the DEGs of the five core genes to the DAVID database. Besides, the cut-off was set as  $P < 0.05$ .

### Hub gene levels and prognostic value

We imported the hub genes in the GEPIA2 database (<http://gepia2.cancer-pku.cn/>) for calculating the prognostic index (Tang et al. 2019). Gene expression profiles in cancer tissues and normal tissues can be studied using this database. Apart from that, the Kaplan-Meier (KM) curve was also plotted with the purpose of evaluating the prognostic outcome for advanced ccRCC cases based on the hub genes.

### Establishing gene-drug interactions

The DGIdb database (<https://dgidb.org/>) was adopted for obtaining the drug-gene interaction data (Freshour et al. 2021). We imported the detected hub genes to this database using GEPIA2 for selecting the compounds or drugs with the filter criteria supported by previous studies and a relationship score  $> 2.0$ .

## Results

### Screening for DEGs

The GSE53757 and GSE66271 datasets were selected according to the filter conditions. GSE53757 has 1,334 DEGs, where 538 were upregulated and 796 were downregulated; GSE66271 has 1,438 DEGs, among which 796 presented upregulation, and 796 showed downregulation (Fig. 1). A Venn diagram was constructed to visualize the intersection of 861 common DEGs, among which 287 were upregulated with 574 being downregulated (Table 2, Fig. 2).

### GO and KEGG functional annotation for DEGs

Concerning the GO-Biological Process (BP) terms, the DEGs were mostly associated with “cell adhesion”, “signal transduction”, “immune response”, “inflammatory response”, “positive cell proliferation regulation”, “neutrophil degranulation”, “negative apoptotic process regulation”, “xenobiotic stimulus response”, “proteolysis”, and “angiogenesis”. In the Cellular Components (CC) annotation, these DEGs were located in the “extracellular exosome”, “extracellular region”, “plasma membrane”, “apical plasma membrane”, “basolateral plasma membrane”, “integral plasma membrane component”, “membrane”, “extracellular space”, “cell surface”, “integral membrane component”, and “external side of the plasma membrane”. In Molecular Function (MF), “oxidoreductase activity”, “protein homodimerization activity”, “protein binding”, “zinc

Table 1. A summary of microarray datasets from Gene Expression Omnibus (GEO) datasets.

Series	Platform	Affymetrix GeneChip	Samples
GSE53757	GPL570	Affymetrix Human Genome U133 Plus 2.0 Array	120
GSE66271	GPL570	Affymetrix Human Genome U133 Plus 2.0 Array	25

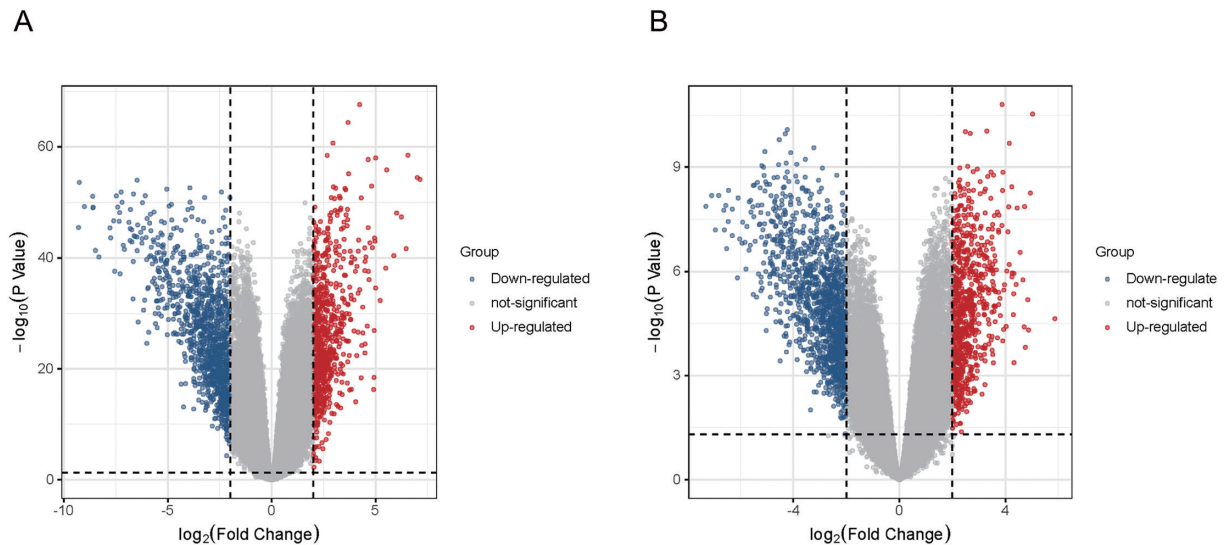


Fig. 1. Volcano plot of differentially expressed genes between advanced clear cell renal cell carcinoma (ccRCC) tissues and normal kidney tissues in datasets GSE53757 and GSE66271. Red denotes genes with high expression in tumor tissues, and blue stands for low expression in tumor tissues. (A) GSE53757; (B) GSE66271.

ion binding”, “identical protein binding”, “receptor binding”, “calcium ion binding”, “macromolecular complex binding”, “transmembrane transporter activity” and “heparin binding” were clustered. Regarding the KEGG analysis, the DEGs were closely related to the pathways of “focal adhesion”, “cytokine-cytokine receptor interaction”, “metabolic pathway”, “phagosome”, the “PPAR pathway”, “cell adhesion molecules”, the “chemokine pathway”, “complement and coagulation cascade”, “carbon metabolism”, and the “interaction between the viral protein and cytokine/cytokine receptor”. The top 20 DEGs associated with the BP, CC, and MF enrichment results and the top 10 DEGs associated with the KEGG pathway were sorted by counts and are shown in Fig. 3.

#### Construction of the protein-protein interaction network

The Cytoscape software was adopted for establishing a PPI network for DEGs from the STRING database. By analyzing the PPI network, the 10 most significant hub genes (*ASPM*, *TPX2*, *DLGAP*, *NCAPG*, *MCM10*, *BIRC5*, *BUB1*, *MELK*, *RRM2*, and *TOP2A*) of advanced ccRCC were detected with the Cytoscape plug-in cytoHubba. Five modules with the highest significance were acquired using the MCODE plug-in. The default conditions were used for all parameters (Fig. 4).

#### Functional enrichment analysis of the core genes

For the GO-BP terms, the five core genes were mostly associated with “cell division”, “chromosome segregation”, “cell cycle”, “apoptosis process”, “protein phosphorylation”, “cell proliferation”, “mitotic cytokinesis”, “DNA repair”, “DNA damage stimulus response of cells”, “immune response”, “signaling”, and “inflammatory reaction”. In the CC annotation, these genes were located in the

“nucleus”, “nucleoplasm”, “cytosol”, “membrane”, “mid-body”, “kinetochore”, “microtubule”, “chromosome”, the “centromeric region”, “centrosome”, “plasma membrane”, “extracellular region”, and the “cell surface”.

In the MF terms, “protein homodimerization activity”, “protein kinase binding”, “ATP-dependent microtubule motor activity, plus-end-directed”, “protein binding”, “microtubule binding”, “ATP binding”, “microtubule motor activity”, “identical protein binding”, “chemokine activity”, “receptor binding”, “heparin binding” as well as “transmembrane signaling receptor activity” were clustered.

Regarding the KEGG analysis, “metabolic pathways”, the “Toll-like receptor pathway”, the “chemokine pathway”, the “Rap1 pathway”, the “PI3K-Akt pathway”, the “interaction between cytokine and cytokine receptor”, the “interaction between the viral protein and cytokine/cytokine receptor”, “focal adhesion”, “Coronavirus disease-COVID-19”, the “HIF-1 pathway”, “Human papillomavirus infection”, and the “Natural killer cell-regulated cytotoxicity” pathways were closely related to these core genes. The top 10 GO annotations and KEGG pathway enrichment were sorted by counts and are shown in Fig. 5.

#### Verification and survival analysis

We analyzed the survival relevance of the amplified genes to further identify the prognostically relevant genes that might inhibit advanced ccRCC. By using the GEPIA database, we analyzed how hub genes affect the survival of ccRCC. The *BIRC5*, *BUB1*, *MELK*, *RRM2*, *TOP2A*, and *TPX2* levels showed obvious association with the overall survival of the patients (Fig. 6). Apart from that, the overall survival rate of ccRCC patients was reduced considerably when hub genes were upregulated ( $P < 0.05$ ) (Fig. 7).

Table 2. The common differentially expressed genes (DEGs).

DEGs	Gene names
Up-regulated	<p> <i>PNCK XCL1 KCNMA1 E2F8 STK10 ITGA5 MYBL1 PARVG PFKP CXCR4 NCF4 CRTAM CSPG4 CD163 CD37 IDO1 MSC-AS1 TPX2 EPHA3 RAB42 LILRB2 C1QC FLT1 IGF2BP3 TRIB3 TYROBP IKBIP CCL18 ASPM AXL TRAC PML KCN3 NETO2 DOCK2 CENPE FPR3 CXCL13 FAP LOC100509445 ALOX5 PLK2 CDH13 ANGPTL4 ARHGAP9 DDIT4 PTPN22 INHBA RUNX3 PIK3R5 HIGD1B LOXL2 PGF LILRB1 ARL11 COL1A1 RAC2 ADAMDEC1 GPD5 SAMHD1 ANLN FAM57A BIRC5 TMEM45A TREM2 MS4A4A DDB2 MIR6787 EGFR PLEKHO1 IKZF1 DUSP4 LAIR1 SLITRK5 EVI2A FOXM1 LGALS1 FXYD5 ST8SIA4 NCF1C C3 FCGR1CP TLR7 CHST15 CLEC7A LAMP3 FABP5 CLEC2B TNFSF13B LOC100509457 YME1L1 SAP30 CEP55 SLC2A3 PTHLH CD36 FCGR2C BIN2 CORO1A RRM2 HK2 PAG1 DCLK1 SLC35F6 TOP2A TFR2 FYB CXCL9 CAV1 FANCI CCL28 ZNF395 NRP2 ARL4C ISG20 PLEKHG2 TMEM44 CD300A AKNA CXCL11 SLFN13 C1QB ADAMTS2 TRAC SIGLEC10 FCGR1B MIR155 GZMK CD70 KISS1R LRRC25 KIF14 HEY1 FN1 SLAMF7 MIR1204 OLFML2B MS4A6A DLGAP5 INPP5D NKG7 FABP6 NOL3 TAGAP IFI16 CDCA7L CSTA CXCL10 MS4A7 RRAD TNFAIP6 NDUFA4L2 LCP2 SERPINE1 VCAN SLFN11 SLC16A1-AS1 KLHL6 TNFRSF4 SLC1A3 NPTX2 TRPV2 CCL5 DTL ENTPD1 CTSS EHBPI1 LOC101927345 MIR6756 LOX PDK1 CDCA2 VSIG1 FLJ32255 FKBP10 CMC4 CLEC2D CD300LF RNASET2 CD84 TLR8 CXCL5 LAPT5 GJC1 C5orf46 LOC101928269 SCD HSPA6 FBXO16 ADM HILPDA CCR5 STAMBPL1 SLAMF8 MYO1G CA9 TRPA1 EGLN3 ENO2 CSF2RA CHSY3 KIF20A LOC102724660 FAM49A EHD2 CLEC4A MCM10 CAV2 CENPK IL21R SOX11 P2RY12 VWF IGSF6 IL4I1 STC2 DUSP5P1 SIGLEC1 MSR1 CCL4 FCER1G LAT2 TRBC1 IGFBP3 LOC101928916 CDCA7 C1QA PFKFB4 MELK PPF1A4 NOD2 ADGRE2 HES4 GBP5 LOC101060835 ITGB2 TRIM9 CDKN2B CTHRC1 UHRF1 APOL1 P2RX7 SCARBI AHNAK2 GRAMD4 FCGR3B KIAA1010 TGFB1 TIMP1 INHBB ABCA12 PLOD2 PLXDC1 PLAUR BUB1 BHLHE41 GIT2 SPAG4 NUF2 NCAPG CD86 LPCAT1 COL1A2 CP ARHGAP22 PRR11 IBSP NNMT ADA KCNE4 FAM26F APOC1 PYCARD NEK2 CENPM VAV1 THEMIS DUXAP10 RGS1 MIR210HG ACKR3 HAPLN1 ANGPT2 BIRC3 DEPDC1 PTPRC ITGA4</i> </p>
Down-regulated	<p> <i>PTGER3 ERBB4 RALYL DNASE1 XPNPEP2 SLC5A11 SLC4A1 CADM4 ACOT12 SLC17A1 MPPED2 EHF TMC4 ARSF KLK6 LOC105377924 NAPIL2 HMGCS2 RENBP KLHL14 LOC389332 PROZ REEP6 LOC101930168 HRG CAPN3 TCL6 KCNE1 GDA LDHD SLC15A2 SERPINA6 LINC00645 UGT3A1 GK SLC13A1 TMEM174 LOC105375115 LRRN2 MYO3B PROM2 TMEM132E CALB1 BIK SUSD2 SUGCT SFXN2 KIAA2022 AMBP HSD11B2 TUBAL3 ZYG11A DEFB1 ACSM3 NOS1 CLDN11 CRYM ACSBG2 GPC5 LOC149703 TRPM6 CPNE4 LOC149684 CLDN16 DACHI SHISA3 MPP7 ANO5 APOC3 TMEM30B SMIM22 BHMT ANGPTL3 MAOA ZNF385B ETNK2 ADGRF1 TFCP2L1 PAK6 ALDH4A1 TSPAN8 CPEB3 KLRG2 KL PKLR QPRT TDGF1P3 PDZD3 SLC22A6 GPD1 C1orf168 SLC12A6 EFHD1 LOC100505985 PCK2 TOX3 CRHBP AQP2 ASS1 ALAD DAO C9orf66 PLXNB1 AZGP1P1 GRIK2 IGSF11 MRLN CCDC181 MIOX PIGR ATP6V1G3 FUT6 STRIP2 FOLR1 CLSTN2 SCD5 MAL SEBOX FGF1 VTCN1 TFAP2B PAPP A INPP5J PLA2R1 CEL ENAM MT1M TNNC1 COL4A3 NPHS1 IL1RL1 SYNE4 CYP4F3 SLC39A5 MTPP LONRF2 ESRRG KCNJ13 AKR7A3 GRHL2 PTGER1 NDNF PBX1 ABCB1 VGLL1 TMEM252 MPC1 SLC34A1 FAM169A STAP1 MUC15 ANXA9 NR1I3 ACSF2 MT1G ABCA8 KCN10 WTI RALGPS1 UPP2 MFS4A SLC22A8 PHF21B RALGAP2 CRABPI SIM1 GC ADRB1 ALDH6A1 SLC34A3 GSTO2 CHL1 SLC13A2 SLC16A9 TCF21 LRRC2 TPTEP1 EGF SLC51B FAM3B HOGA1 ANK2 RIMBP2 UGT1A3 AOC1 UPK1B TYRP1 MAN1C1 TMPRSS4 MARVELD3 HS6ST2 GLYATL1 STK32A RASSF10 LRP1B TNNT2 LGSN BMP7 SLC25A34 RAB11FIP3 TRIM63 PCK1 SLC26A4 ADHIC IRX1 DPYS GCM1 RNF150 NOX4 WNK4 SGK2 PIK3C2G TMEM72 ACY1 PRR15L LINC01314 PAPP2 CHDH CLDN10 SOST TAC1 STK33 LRRC19 IL17RB PLCXD3 SCNN1B GABRA2 ZNF750 USP2 SLC52A3 GRM1 PLCD4 KCNH6 FCAMR CLIC5 LINC00982 ESRRB KCNJ10 NPNT PRAP1 AFM CSMD1 RAB25 MAP6 ACPD HPGD DNAJC12 FXFD4 CCDC160 AIF1L PPM1E MME CWH43 RHCG THRSP CYP4A11 OSBPL6 AGXT2 TMEM207 GGT6 LOC101928047 FMO1 C7 GP2 AQP6 TMEM178A COCH MST1L SLC30A2 LZTS3 LIX1 FREM2 C9orf135 CLCNKB APOM SLC7A8 GLTPD2 PDE1A TMPRSS2 CYP2B6 DPP6 FAM151A EPCAM ANGPTL1 RHBG EMX1 MRO PCSK1N AJAP1 PROC ATP6V0A4 ENTPD5 LHX1 SMIM24 CYP4A22 CDH3 CLNK LYPD6B PLPP4 CNTN3 CHGB VIL1 ETNPPL SORCS1 PACRG SLC23A1 HPD GGACT SLC7A13 TMEM45B CSDC2 FLJ22763 PAH DNMT3L ATP2C2 PNPLA3 GATA3 CHP2 PTPRD KCNJ1 LOC285556 SLC12A3 TCEAL2 SLC5A12 SLC5A7 CRYAA ACADSB FAM83B SLC28A2 RBP4 ZNF44 PFKFB2 TTC36 CA4 LOC101927244 SLC2A12 EPN3 KLK7 CYP27B1 OLFM4 CDH9 LINC00551 FABP1 CDH16 NKAIN4 COL4A4 SLC22A7 LOC100130691 ACOT11 CYP4F2 MTURN NELL1 FGF9 APOH PLCL1 NPHS2 C14orf37 ASPDH PALM3 PSAT1 FUT3 SLC4A9 NAPSA SLC6A19 SLC12A1 SCN2A ERP27 ALDH8A1 MCOLN3 CNTN1 LOC284578 SLC7A9 AZGP1 EDDM3A RBM11 SLC22A13 DDN CA10 RDH12 GABRP TACSTD2 OXGR1 C16orf89 LOC100505938</i> </p>

*PRR15 PVALB WDR72 FOXI1 ABAT TMEM52B FMO5 RAPGEF3 PAQR5 ANKRD2 SHROOM3 CPNE6 IRX2 ACAA1 ERICH4 RASL11B SEMA6D MYCN CASZ1 S100A2 GATA5 PC SORD DMRT2 LOC727944 GLDC FBP1 LOC101928303 GATA3-AS1 BEX1 WNK3 SPTBN2 PLPPR1 GLYAT SUS4 DDC PRLR GSTM3 HYKK TST CGNL1 SLC47A2 TREH NTNG1 KNG1 CASR MT1HL1 NR0B2 TFAP2A KRT7 SKIDA1 PTPRO OTOGL CLCNKB DPEP1 CYP17A1 MSRA ALDH1A2 TSPAN1 SCN7A RBMY1J ESRP1 TNNI1 PCDH9 TRPM3 PLG SLC7A7 IYD LINC00955 HAO2 ATP6V1C2 CR2 SLC29A2 MTIF DHDH SMIM5 LINC01187 LOC100506459 MYH8 TMEM213 ERVMER34-1 LOC100130278 DCXR UMOD ADH1B ATP6V0D2 WISP3 DIO1 SMC03 ELF5 AP1M2 GABARAPL3 GCAT ACSL6 SCNN1A SIM2 CNDP1 SOSTDC1 ENPP6 PCP4 GPC3 C1orf56 CLDN8 PLG PPP1R1A SLC22A12 CYP2B6 SOWAHA EYA4 SHISA2 KLK1 CYP4F2 SLC5A2 KCNMB2 SLC27A2 CGN MUC13 BMPR1B G6PC RMST XYLB ADH6 AGXT LOC645321 BSND MT1H HEPACAM2 FRMD7 DDX25 SOBP SH3GL2 LOC101929480 ABCC6 ARHGAP24 TMEM61 ALB FREM1 ALDOB DLK1 SCNN1G SLC13A3 CYP8B1 LOC101928658 SLIT2 FTCD BSPRY SUCNR1 CBLC DNER PLEKHA5 ADGRV1 SALL3 ACOX2 CPN2 AGMAT KCNJ15 CTXN3 NRK PTH1R C1orf116 SLC26A7 PHYHD1 RPRM GATM EPB41L5 RNF212B OGDHL C2orf40 ATP6V1B1 SLC25A48 AOX1 DUSP9 SERPINA5 SFRP1 GLOD5 PIPOX GPAT3 FMN2 PRODH2 PEPD NXPH2 SLC16A10 HYAL1 ST18 AGR2 HECW1 TRIM50 HOXB-AS3 LOC643923*

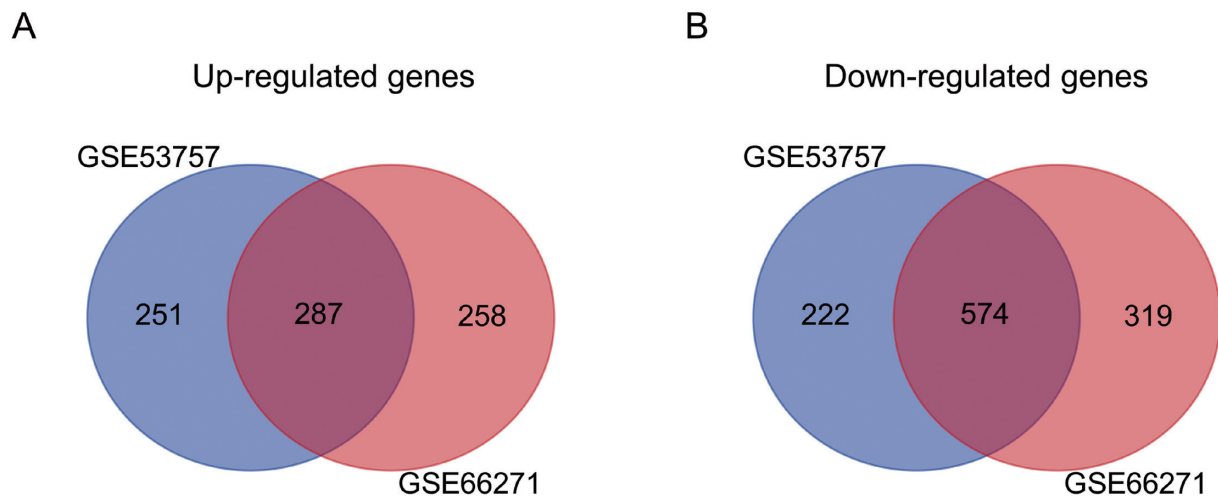


Fig. 2. Venn diagram to intersect differentially expressed genes (DEGs) of advanced ccRCC. (A) Common up-regulated DEGs, totally 287. (B) Common down-regulated DEGs, a total of 574.

#### Establishing the gene-drug interaction

In order to investigate the correlation between genes and drugs, the six verified hub genes were uploaded to the DGIdb database. We only identified *RRM2* and *TOP2A* and matched them with three estimated therapeutic agents (gallium nitrate, cladribine, and amonafide) (Table 3). The filter criteria included a relationship score > 2.0 and being supported by previous studies (Table 4).

#### Discussion

RCC mainly includes ccRCC, chromophobe RCC, and papillary RCC (Ljungberg et al. 2019). CcRCC belongs to one of the deadliest subtypes of urinary malignancy and has the highest tumor metastasis rate, recurrence rate, and mortality rate among histological subtypes of RCC (Patard et al. 2005). It is found that the prognosis of advanced ccRCC is poor with its five-year survival rate being as low as 11.7% (Siegel et al. 2017). Radiotherapy or chemotherapy has no significant effect on ccRCC patients; the most effective

treatment method is surgical resection (Makhov et al. 2018). However, postoperative metastasis in patients with ccRCC is as high as 30%. The survival rate of patients with metastasis or preoperative metastasis is low, and the average survival time is less than one year (Hsieh et al. 2017). Therefore, elucidating the pathogenesis of highly advanced ccRCC is necessary, as it might help to develop clinical therapeutic strategies for ccRCC and identify the potential molecular targets for ccRCC-targeted drugs. Based on the quick progress of bioinformatics, a lot of microarray and sequencing data are available, which can be adopted for diagnosing and identifying treatment targets for various diseases (Batai et al. 2018; Martinez-Romero et al. 2018). Bioinformatics methods have been recently used to conduct secondary analysis of ccRCC-related data to identify the candidate genes of ccRCC (Yuan et al. 2018). In the current work, we explored gene-drug prediction in more detail to identify potential drugs that might be used for treating advanced ccRCC and provide new ideas for other studies.

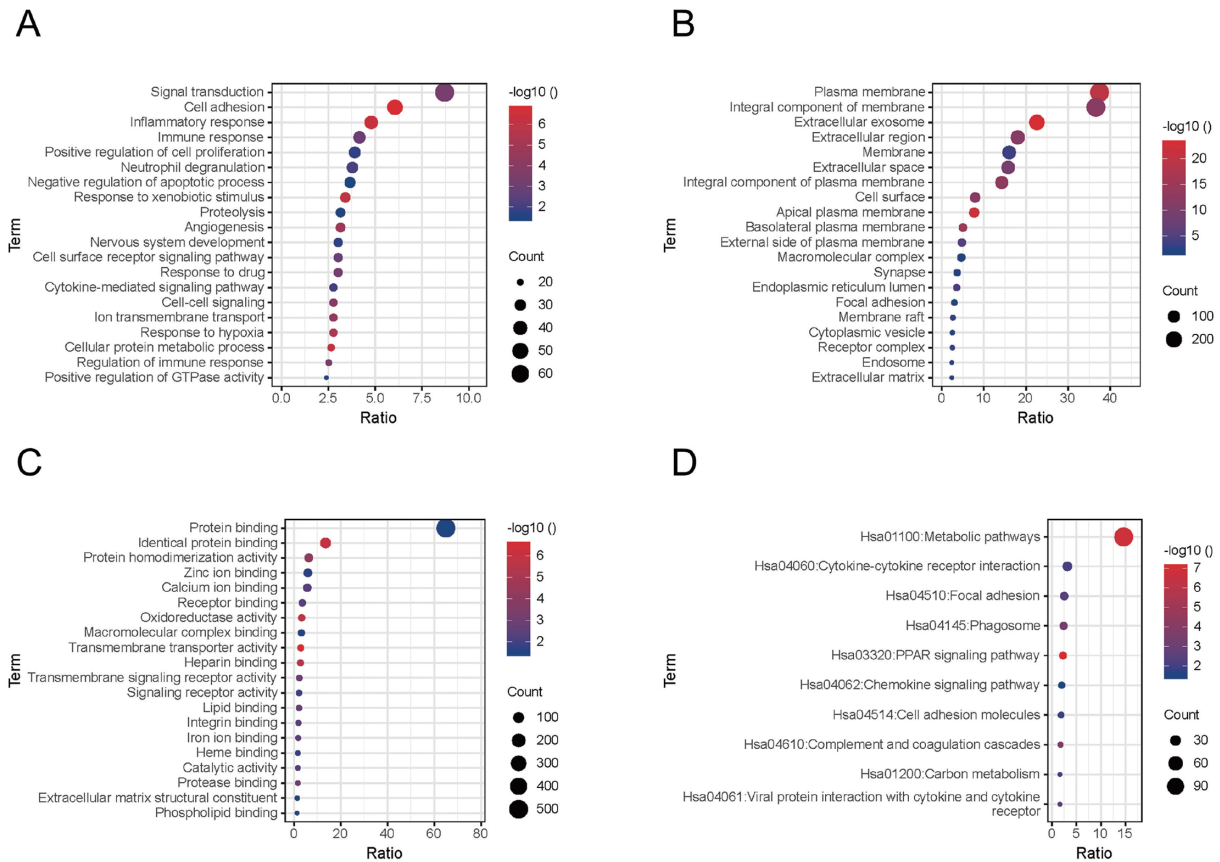


Fig. 3. The Gene Ontology (GO) annotation and Kyoto Encyclopedia of Genes and Genomes (KEGG) analysis of DEGs bubble plots. The results of top 20 GO annotation and the top 10 KEGG analysis were presented. (A) Biological process; (B) Cellular component; (C) Molecular function; (D) Signal pathway.

Two datasets, GSE53757 and GSE66271, were analyzed online through GEO2R to identify DEGs in advanced ccRCC compared to healthy renal tissues. Then, we used various bioinformatics analysis methods to analyze the DEGs for a better understanding of these genes based on GO annotation, the KEGG enrichment analysis, and the PPI network analysis. Then, we performed verification, gene-drug interaction, and survival analyses on the hub genes. Our study was the first one to find three drugs (gallium nitrate, cladribine, and amonafide) associated with advanced ccRCC through bioinformatics methods. Our findings might provide new treatment strategies for advanced ccRCC patients.

In this study, we obtained 861 DEGs (287 were upregulated and 574 were downregulated). In BP annotation, the DEGs were primarily associated with “cell adhesion”, “signaling”, “inflammatory reaction”, “immune response”, “positive cell proliferation regulation”, “neutrophil degranulation”, “negative apoptotic process regulation”, and “xenobiotic stimulus response”. Regarding the CC terms, the DEGs were mostly associated with “basolateral plasma membrane”, “apical plasma membrane”, “external side of the plasma membrane”, “cell surface”, “membrane component”, “plasma membrane”, “membrane”, and “plasma

membrane component”. In MF annotation, these DEGs were predominantly related to “identical protein binding”, “protein binding”, “calcium ion binding”, “zinc ion binding”, “receptor binding”, “heparin binding”, and “macromolecule complex binding”. As revealed by the KEGG enrichment analysis, the common DEGs were predominantly concentrated in “metabolic pathway”, “PPAR signaling pathway”, “carbon metabolism”, “chemokine pathway”, “interaction of cytokine with cytokine receptor”, and “interaction between the viral protein and cytokine/cytokine receptor”.

Based on the PPI network, five core gene groups with the most stable structures were extracted. Then, we identified the hub genes that might be essential drug targets for advanced ccRCC and used Venn diagrams to visualize the top 10 common genes and gene clusters. We found that the 10 most significant genes were the hub genes. Thus, we analyzed the genes of the core groups with GO and KEGG. These core genes were mostly associated with the immune and inflammatory responses of the biological process. The upregulated DEGs of ccRCC were primarily involved in inflammatory and immune responses (Zhang et al. 2019; Xu et al. 2020). Regarding the cellular components, the DEGs were mainly associated with the membrane; this was

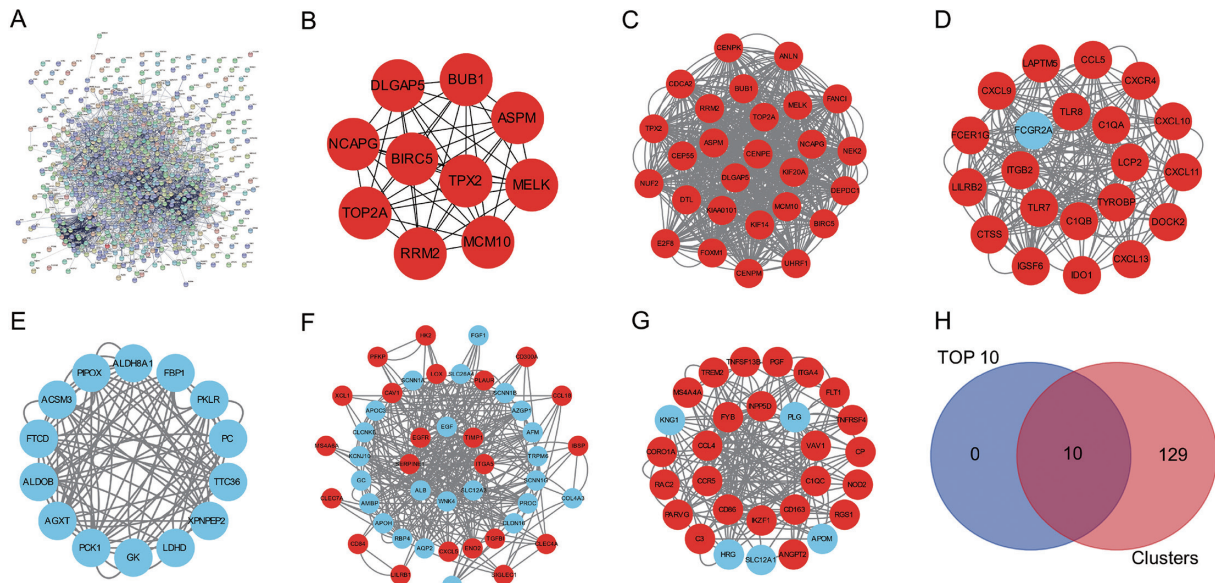


Fig. 4. Module analysis from the protein-protein interaction (PPI) network. By adopting Cytoscape software, the top 10 genes and the five most stable core gene groups in the network were screened from the protein-protein network. Red signifies up-regulated genes, and blue stands for down-regulated genes. A Venn diagram was adopted for visualizing the top 10 genes contained in the five core gene groups. (A) PPI enrichment map, with 717 nodes and 8,110 edges; (B) Top 10 genes, with ten nodes and 45 edges; (C) Core gene cluster 1, with 27 nodes and 676 edges; (D) Core gene group 2, with 14 nodes, 234 edges; (E) Core gene group 3, with 14 nodes, 92 edges; (F) Core gene group 4, with 46 nodes, 296 edges; (G) Core gene group 1, with 29 nodes and 168 edges; (H) Venn diagram to visualize the common genes of top 10 and clusters. (B) is the top 10 genes which gets from the cytoHubba plug-in, while (C-G) are the core gene groups which get from the MCODE plug-in of the Cytoscape.

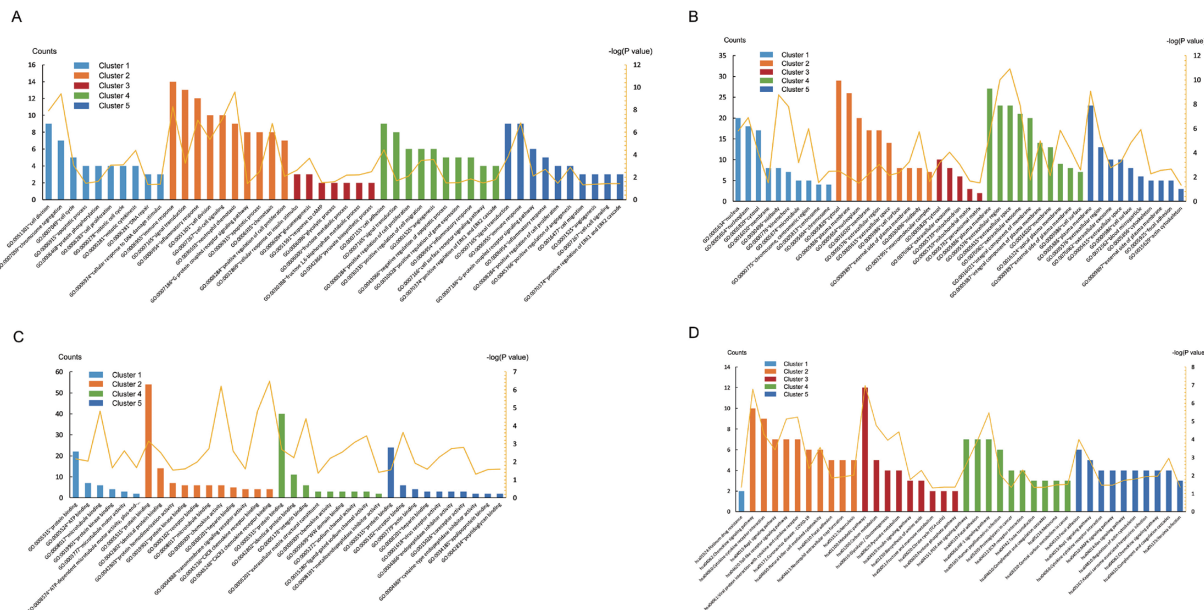


Fig. 5. Two-coordinate graph of Gene Ontology (GO) annotation and Kyoto Encyclopedia of Genes and Genomes (KEGG) enrichment analysis of differentially expressed genes (DEGs) in each core gene group. The light blue represents core gene group 1; the orange represents core gene group 2; the red represents core gene group 3; the green represents core gene group 4; the dark blue represents core gene group 5; and the yellow curve represents  $-\log_{10}(P\text{-value})$ . (A) Biological process; (B) Cellular component; (C) Molecular function; (D) Signal pathway.

also found by Wang et al. (2020). The upregulated genes of ccRCC are mainly located on the plasma membrane (Quan et al. 2021). Chen et al. (2020) concluded that the DEGs of

ccRCC are also enriched in the nucleus (“nucleus” and “kinetochore”), and this observation was similar to the findings of our study. Similar to the results of Quan et al.

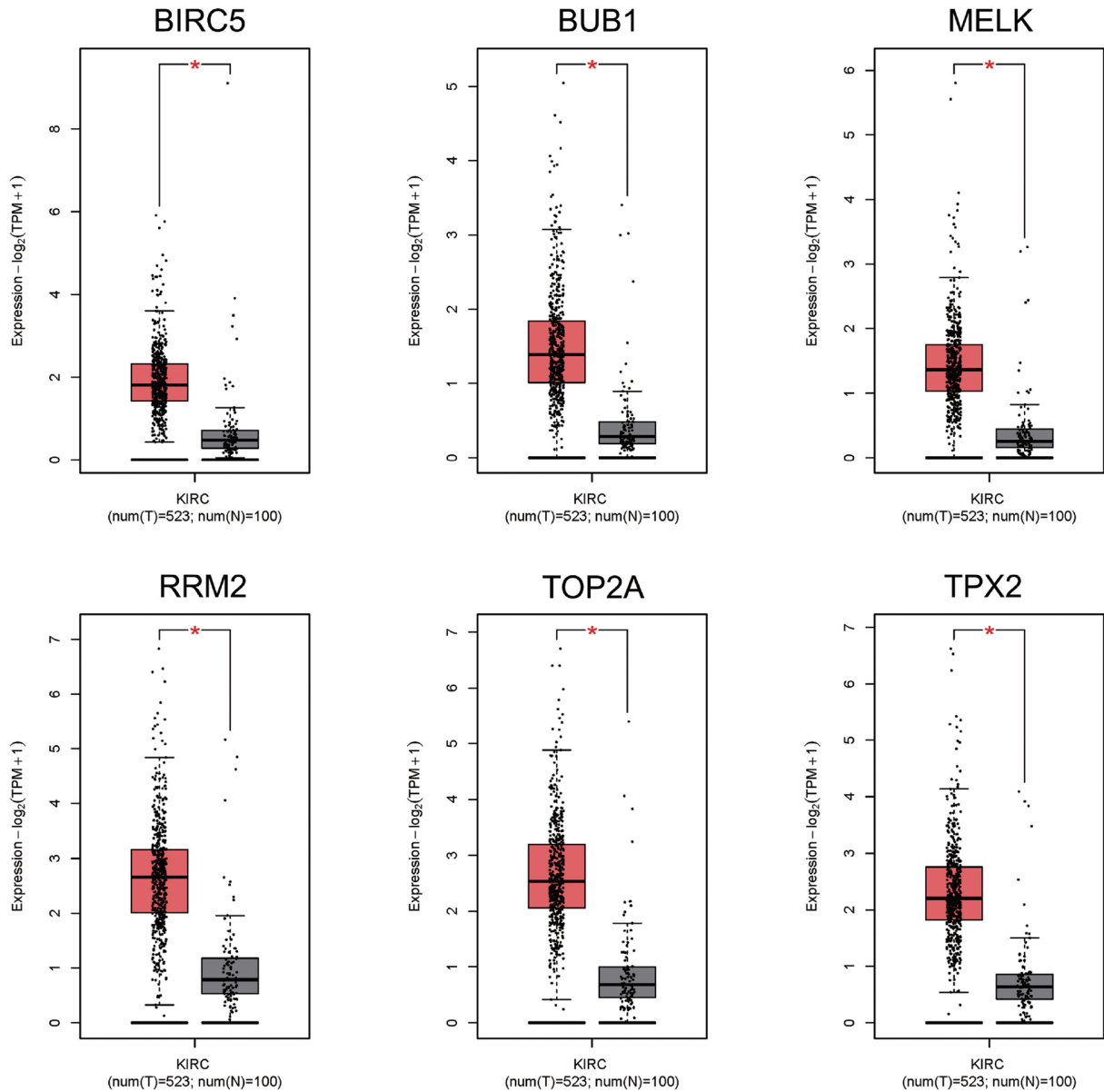


Fig. 6. Boxplots for validating the hub gene for clinical data validation of tumor and normal kidney tissue from advanced ccRCC patients.

\* $P < 0.05$ . Red represents advanced ccRCC tissue, and gray represents normal kidney tissue.

(2021), we found that the molecular functions of the DEGs in advanced ccRCC were associated with the binding function of proteins and metal ions. Several studies have also verified this finding (Wang et al. 2020). The KEGG pathway of the core genes included the “PI3K-Akt pathway”, the “interaction of cytokine with cytokine receptor”, and “focal adhesions”. In some studies, the above three pathways were shown to be related to and have an important effect on ccRCC progression (Wang et al. 2019; Zhou et al. 2019).

The hub genes were introduced into GEPIA2 for further verification. Besides, the expression of the 10 hub genes remained unchanged after confirmation by the TCGA database. The differential expression of six genes (*BIRC5*, *BUB1*, *MELK*, *RRM2*, *TOP2A*, and *TPX2*) was statistically

significant between the ccRCC samples and standard kidney samples. Moreover, according to survival analysis, upregulation of these hub genes would lower the overall survival rate of patients, suggesting a close association of such hub genes with the progression of ccRCC. Gene-drug interaction analysis was performed on the six verified hub genes. Only three small-molecule drugs (gallium nitrate, cladribine, and amonafide) were found to be associated with *RRM2* and *TOP2A*.

The *RRM2* protein belongs to one of the subunits of the nucleotide reductase complex that catalyzes the formation of deoxynucleotides and exerts a vital function in DNA synthesis. It is associated with tumor growth, angiogenesis, invasion, metastasis, and patient prognosis (Chen et al. 2019). Thus, it is the efficient anti-tumor target enzyme.

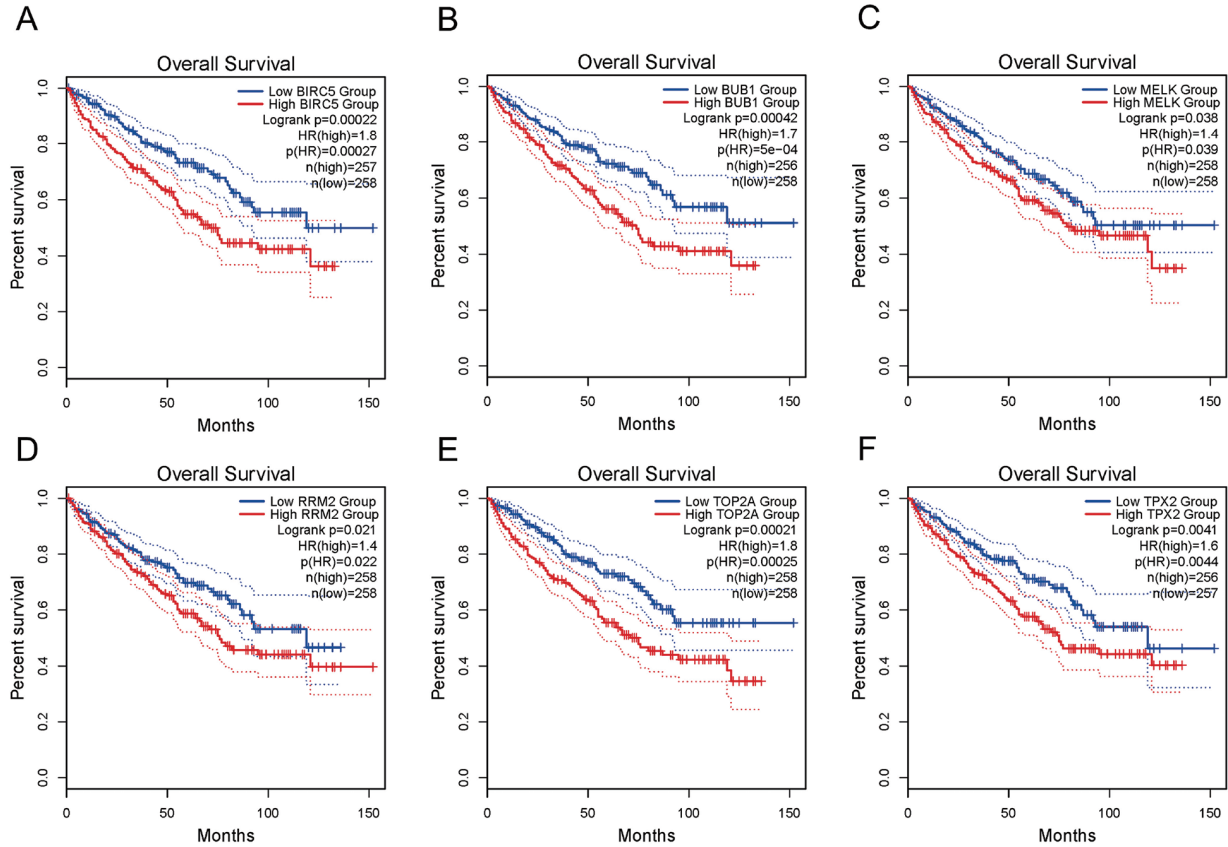


Fig. 7. The overall survival curve of the hub gene was drawn with the use of the GEPIA platform.  $P < 0.05$  was regarded to show statistical significance. The survival curve indicated that in advanced ccRCC patients, patients with high expression of up-regulated hub genes had a shorter survival time. Red stands for high gene expression with blue representing low gene expression. (A) *BIRC5*, (B) *BUB1*, (C) *MELK*, (D) *RRM2*, (E) *TOP2A*, (F) *TPX2*.

Table 3. The effective drugs targeted hub genes.

Gene names	Interaction type	Drug names	Interaction score
<i>RRM2</i>	Inhibitory	Gallium nitrate	6.53
	Inhibitory	Cladribine	2.28
<i>TOP2R</i>	N/A	Amonafide	2.78

N/A, Not Applicable.

Table 4. Publications associated with the effective drugs targeted hub genes.

Gene names	Drug names	Publications
<i>RRM2</i>	Gallium nitrate	Chitambar 2004; Narasimhan et al. 1992; Straus 2003
	Cladribine	Cao et al. 2013; Kantarjian et al. 2007; Kline and Larson 2005; Sampat et al. 2009; Takahashi et al. 1999; Zhenchuk et al. 2009
<i>TOP2R</i>	Amonafide	Chen et al. 2010; Quintana-Espinoza et al. 2013; Tan et al. 2013; Tan et al. 2015; Van Quaquebeke et al. 2007

*RRM2* upregulation is tightly related to the genesis and development of different types of cancer, like gastric cancer (Kang et al. 2014), colorectal cancer (Hsieh et al. 2016), non-small cell lung cancer (Mah et al. 2015), and nasopharyngeal cancer (Han et al. 2015). Moreover, in the genitourinary system, studies have also demonstrated that upregu-

lation of *RRM2* may reduce bladder cancer (Morikawa et al. 2010) and adrenocortical cancer (Grolmusz et al. 2016) survival. The findings of the current work suggested that *RRM2* can be applied as a potential biomarker of advanced ccRCC. Some studies also found that the expression of *RRM2* associates with Fuhrman grading and the pathologi-

cal stage (Zou et al. 2019). On the contrary, knockout of the *RRM2* gene leads to ccRCC cell line arrest, thereby inhibiting tumor growth (Osako et al. 2019).

*TOP2A* has an important effect on the topological state of DNA during replication and transcription. The occurrence of cancer is inseparable from the process of DNA metabolism. Being an enzyme that plays an irreplaceable role in gene expression, *TOP2A* is closely related to diverse categories of cancer including pancreatic cancer (Pei et al. 2018) and gastric cancer (Terashima et al. 2017). In cell carcinoma, *TOP2A* is associated with renal papillary carcinoma (Ye et al. 2018) and renal clear cell carcinoma (Zhang et al. 2019). The expression of *TOP2A* in renal clear cell carcinoma relates to a pathological stage that might result in the progression of renal cell carcinoma (Chen et al. 2018). Thus, *TOP2A* might become a new prognostic marker for RCC.

Anti-tumor drugs act in various ways, but the cornerstone of cancer therapy is DNA-targeting. Through gene-drug interaction analysis, gallium nitrate and cladribine were identified as inhibitors of *RRM2*. Amonafide is related to *TOP2A*, but the relationship is not clear. Gallium is a metal that is pharmacologically similar to iron. It can inhibit ribonucleotide reductase by replacing iron in its M2 subunit, leading to the loss of a tyrosyl radical, thereby inhibiting ribonucleotide reductase activity, DNA synthesis, and tumor growth (Narasimhan et al. 1992). Gallium nitrate can inhibit *RRM2* and, thus, might be a potential drug for advanced ccRCC (Chitambar 2004). Cladribine refers to a synthetic purine nucleoside analog that promotes lymphocyte depletion mainly by continuously reducing B lymphocytes (Jacobs et al. 2018; Pfeuffer et al. 2022). Cladribine was initially used for hematological diseases (Beutler 1992). It can also be administered for treating other conditions, such as multiple sclerosis (Giovannoni et al. 2018) and cervical cancer (Yi et al. 2019). Nevertheless, no study has investigated the effect of cladribine on ccRCC. Cladribine might have an inhibitory effect on the *RRM2* gene, and thus, it might inhibit advanced ccRCC (Zhenchuk et al. 2009; Cao et al. 2013). Amonafide induces apoptosis by intercalating DNA and blocking the binding of Topo II to DNA (Allen and Lundberg 2011). It can treat acute myeloid leukemia (Freeman et al. 2012) and breast cancer (Costanza et al. 1995). It is found that the mechanism of action of amonafide shows relationship to *TOP2A* (Quintana-Espinoza et al. 2013; Tan et al. 2015). Although the correlation is unclear, it might be a potential targeted drug for ccRCC.

This study had some limitations. First, bioinformatics analyses were conducted without experimental verification. Second, there was a specific risk of bias. Finally, the screened hub genes and drugs need to be verified empirically.

In conclusion, through bioinformatics analysis, we found that *RRM2* and *TOP2A* have an important effect on the genesis, progression and prognostic outcome of

advanced ccRCC. Thus, they might serve as novel diagnostic and therapeutic biomarkers. Three identified drugs (gallium nitrate, cladribine, and amonafide) might be administered for the treatment of advanced ccRCC.

### Acknowledgments

We appreciate for all the public databases and websites applied in the present study. This study was supported by the Fujian Provincial Nature and Science Foundation (Grant No. 2020J011206).

### Conflict of Interest

The authors declare no conflict of interest.

### References

- Allen, S.L. & Lundberg, A.S. (2011) Amonafide: a potential role in treating acute myeloid leukemia. *Expert Opin. Investig. Drugs*, **20**, 995-1003.
- Barrett, T., Wilhite, S.E., Ledoux, P., Evangelista, C., Kim, I.F., Tomashevsky, M., Marshall, K.A., Phillippy, K.H., Sherman, P.M., Holko, M., Yefanov, A., Lee, H., Zhang, N., Robertson, C.L., Serova, N., et al. (2013) NCBI GEO: archive for functional genomics data sets—update. *Nucleic Acids Res.*, **41**, D991-995.
- Batai, K., Imler, E., Pangilinan, J., Bell, R., Lwin, A., Price, E., Milinic, T., Arora, A., Ellis, N.A., Bracamonte, E., Seligmann, B. & Lee, B.R. (2018) Whole-transcriptome sequencing identified gene expression signatures associated with aggressive clear cell renal cell carcinoma. *Genes Cancer*, **9**, 247-256.
- Beutler, E. (1992) Cladribine (2-chlorodeoxyadenosine). *Lancet*, **340**, 952-956.
- Cao, L., Chen, Y., Zhang, M., Xu, D.Q., Liu, Y., Liu, T., Liu, S.X. & Wang, P. (2018) Identification of hub genes and potential molecular mechanisms in gastric cancer by integrated bioinformatics analysis. *PeerJ*, **6**, e5180.
- Cao, X., Mitra, A.K., Pounds, S., Crews, K.R., Gandhi, V., Plunkett, W., Dolan, M.E., Hartford, C., Raimondi, S., Campana, D., Downing, J., Rubnitz, J.E., Ribeiro, R.C. & Lamba, J.K. (2013) *RRM1* and *RRM2* pharmacogenetics: association with phenotypes in HapMap cell lines and acute myeloid leukemia patients. *Pharmacogenomics*, **14**, 1449-1466.
- Chen, J.Y., Sun, Y., Qiao, N., Ge, Y.Y., Li, J.H., Lin, Y. & Yao, S.L. (2020) Co-expression network analysis identifies fourteen hub genes associated with prognosis in clear cell renal cell carcinoma. *Curr. Med. Sci.*, **40**, 773-785.
- Chen, L., Yuan, L., Qian, K., Qian, G., Zhu, Y., Wu, C.L., Dan, H.C., Xiao, Y. & Wang, X. (2018) Identification of biomarkers associated with pathological stage and prognosis of clear cell renal cell carcinoma by co-expression network analysis. *Front. Physiol.*, **9**, 399.
- Chen, W.X., Yang, L.G., Xu, L.Y., Cheng, L., Qian, Q., Sun, L. & Zhu, Y.L. (2019) Bioinformatics analysis revealing prognostic significance of *RRM2* gene in breast cancer. *Biosci. Rep.*, **39**, BSR20182062.
- Chen, Z., Liang, X., Zhang, H., Xie, H., Liu, J., Xu, Y., Zhu, W., Wang, Y., Wang, X., Tan, S., Kuang, D. & Qian, X. (2010) A new class of naphthalimide-based antitumor agents that inhibit topoisomerase II and induce lysosomal membrane permeabilization and apoptosis. *J. Med. Chem.*, **53**, 2589-2600.
- Chitambar, C.R. (2004) Apoptotic mechanisms of gallium nitrate: basic and clinical investigations. *Oncology (Williston Park)*, **18**, 39-44.
- Costanza, M.E., Berry, D., Henderson, I.C., Ratain, M.J., Wu, K., Shapiro, C., Duggan, D., Kalra, J., Berkowitz, I. & Lyss, A.P. (1995) Amonafide: an active agent in the treatment of previ-

- ously untreated advanced breast cancer--a cancer and leukemia group B study (CALGB 8642). *Clin. Cancer Res.*, **1**, 699-704.
- Dennis, G. Jr., Sherman, B.T., Hosack, D.A., Yang, J., Gao, W., Lane, H.C. & Lempicki, R.A. (2003) DAVID: Database for Annotation, Visualization, and Integrated Discovery. *Genome Biol.*, **4**, P3.
- Dong, D., Mu, Z., Wei, N., Sun, M., Wang, W., Xin, N., Shao, Y. & Zhao, C. (2019) Long non-coding RNA ZFAS1 promotes proliferation and metastasis of clear cell renal cell carcinoma via targeting miR-10a/SKA1 pathway. *Biomed. Pharmacother.*, **111**, 917-925.
- Ferlay, J., Colombet, M., Soerjomataram, I., Dyba, T., Randi, G., Bettio, M., Gavin, A., Visser, O. & Bray, F. (2018) Cancer incidence and mortality patterns in Europe: estimates for 40 countries and 25 major cancers in 2018. *Eur. J. Cancer*, **103**, 356-387.
- Freeman, C.L., Swords, R. & Giles, F.J. (2012) Amonafide: a future in treatment of resistant and secondary acute myeloid leukemia? *Expert Rev. Hematol.*, **5**, 17-26.
- Freshour, S.L., Kiwala, S., Cotto, K.C., Coffman, A.C., McMichael, J.F., Song, J.J., Griffith, M., Griffith, O.L. & Wagner, A.H. (2021) Integration of the Drug-Gene Interaction Database (DGIdb 4.0) with open crowdsourcing efforts. *Nucleic Acids Res.*, **49**, D1144-D1151.
- Giovannoni, G., Soelberg Sorensen, P., Cook, S., Rammohan, K., Rieckmann, P., Comi, G., Dangond, F., Adeniji, A.K. & Vermersch, P. (2018) Safety and efficacy of cladribine tablets in patients with relapsing-remitting multiple sclerosis: results from the randomized extension trial of the CLARITY study. *Mult. Scler.*, **24**, 1594-1604.
- Grolmusz, V.K., Karasz, K., Micsik, T., Toth, E.A., Meszaros, K., Karvaly, G., Barna, G., Szabo, P.M., Baghy, K., Matko, J., Kovalszky, I., Toth, M., Racz, K., Igaz, P. & Patocs, A. (2016) Cell cycle dependent RRM2 may serve as proliferation marker and pharmaceutical target in adrenocortical cancer. *Am. J. Cancer Res.*, **6**, 2041-2053.
- Han, P., Lin, Z.R., Xu, L.H., Zhong, Q., Zhu, X.F., Liang, F.Y., Cai, Q., Huang, X.M. & Zeng, M.S. (2015) Ribonucleotide reductase M2 subunit expression and prognostic value in nasopharyngeal carcinoma. *Mol. Med. Rep.*, **12**, 401-409.
- Hsieh, J.J., Purdue, M.P., Signoretti, S., Swanton, C., Albiges, L., Schmidinger, M., Heng, D.Y., Larkin, J. & Ficarra, V. (2017) Renal cell carcinoma. *Nat. Rev. Dis. Primers*, **3**, 17009.
- Hsieh, Y.Y., Chou, C.J., Lo, H.L. & Yang, P.M. (2016) Repositioning of a cyclin-dependent kinase inhibitor GW8510 as a ribonucleotide reductase M2 inhibitor to treat human colorectal cancer. *Cell Death Discov.*, **2**, 16027.
- Jacobs, B.M., Ammoscato, F., Giovannoni, G., Baker, D. & Schmierer, K. (2018) Cladribine: mechanisms and mysteries in multiple sclerosis. *J. Neurol. Neurosurg. Psychiatry*, **89**, 1266-1271.
- Jia, A., Xu, L. & Wang, Y. (2021) Venn diagrams in bioinformatics. *Brief. Bioinform.*, **22**, bbab108.
- Kang, W., Tong, J.H., Chan, A.W., Zhao, J., Wang, S., Dong, Y., Sin, F.M., Yeung, S., Cheng, A.S., Yu, J. & To, K. (2014) Targeting ribonucleotide reductase M2 subunit by small interfering RNA exerts anti-oncogenic effects in gastric adenocarcinoma. *Oncol. Rep.*, **31**, 2579-2586.
- Kantarjian, H.M., Jeha, S., Gandhi, V., Wess, M. & Faderl, S. (2007) Clofarabine: past, present, and future. *Leuk. Lymphoma*, **48**, 1922-1930.
- Kline, J.P. & Larson, R.A. (2005) Clofarabine in the treatment of acute myeloid leukaemia and acute lymphoblastic leukaemia: a review. *Expert Opin. Pharmacother.*, **6**, 2711-2718.
- Li, M.X., Jin, L.T., Wang, T.J., Feng, Y.J., Pan, C.P., Zhao, D.M. & Shao, J. (2018) Identification of potential core genes in triple negative breast cancer using bioinformatics analysis. *Oncotargets Ther.*, **11**, 4105-4112.
- Ljungberg, B., Albiges, L., Abu-Ghanem, Y., Bensalah, K., Dabestani, S., Fernández-Pello, S., Giles, R.H., Hofmann, F., Hora, M., Kuczyk, M.A., Kuusk, T., Lam, T.B., Marconi, L., Merseburger, A.S., Powles, T., et al. (2019) European Association of Urology Guidelines on Renal Cell Carcinoma: the 2019 Update. *Eur. Urol.*, **75**, 799-810.
- Long, H.P., Liu, J.Q., Yu, Y.Y., Qiao, Q. & Li, G. (2020) PKMYT1 as a potential target to improve the radiosensitivity of lung adenocarcinoma. *Front. Genet.*, **11**, 376.
- Mah, V., Alavi, M., Marquez-Garban, D.C., Maresh, E.L., Kim, S.R., Horvath, S., Bagryanova, L., Huerta-Yepez, S., Chia, D., Pietras, R. & Goodglick, L. (2015) Ribonucleotide reductase subunit M2 predicts survival in subgroups of patients with non-small cell lung carcinoma: effects of gender and smoking status. *PLoS One*, **10**, e0127600.
- Makhov, P., Joshi, S., Ghatalia, P., Kutikov, A., Uzzo, R.G. & Kolenko, V.M. (2018) Resistance to systemic therapies in clear cell renal cell carcinoma: mechanisms and management strategies. *Mol. Cancer Ther.*, **17**, 1355-1364.
- Martinez-Romero, J., Bueno-Fortes, S., Martin-Merino, M., Ramirez de Molina, A. & De Las Rivas, J. (2018) Survival marker genes of colorectal cancer derived from consistent transcriptomic profiling. *BMC Genomics*, **19**, 857.
- Morikawa, T., Maeda, D., Kume, H., Homma, Y. & Fukayama, M. (2010) Ribonucleotide reductase M2 subunit is a novel diagnostic marker and a potential therapeutic target in bladder cancer. *Histopathology*, **57**, 885-892.
- Narasimhan, J., Antholine, W.E. & Chitambar, C.R. (1992) Effect of gallium on the tyrosyl radical of the iron-dependent M2 subunit of ribonucleotide reductase. *Biochem. Pharmacol.*, **44**, 2403-2408.
- Osako, Y., Yoshino, H., Sakaguchi, T., Sugita, S., Yonemori, M., Nakagawa, M. & Enokida, H. (2019) Potential tumorsuppressive role of microRNA99a3p in sunitinibresistant renal cell carcinoma cells through the regulation of RRM2. *Int. J. Oncol.*, **54**, 1759-1770.
- Patard, J.J., Leray, E., Rioux-Leclercq, N., Cindolo, L., Ficarra, V., Zisman, A., De La Taille, A., Tostain, J., Artibani, W., Abbou, C.C., Lobel, B., Guillé, F., Chopin, D.K., Mulders, P.F., Wood, C.G., et al. (2005) Prognostic value of histologic subtypes in renal cell carcinoma: a multicenter experience. *J. Clin. Oncol.*, **23**, 2763-2771.
- Pei, Y.F., Yin, X.M. & Liu, X.Q. (2018) TOP2A induces malignant character of pancreatic cancer through activating beta-catenin signaling pathway. *Biochim. Biophys. Acta Mol. Basis Dis.*, **1864**, 197-207.
- Pfeuffer, S., Rolfes, L., Hackert, J., Kleinschnitz, K., Ruck, T., Wiendl, H., Klotz, L., Kleinschnitz, C., Meuth, S.G. & Pul, R. (2022) Effectiveness and safety of cladribine in MS: real-world experience from two tertiary centres. *Mult. Scler.*, **28**, 257-268.
- Quan, J., Bai, Y., Yang, Y., Han, E.L., Bai, H., Zhang, Q. & Zhang, D. (2021) Bioinformatics analysis of C3 and CXCR4 demonstrates their potential as prognostic biomarkers in clear cell renal cell carcinoma (ccRCC). *BMC Cancer*, **21**, 814.
- Quintana-Espinoza, P., Garcia-Luis, J., Amesty, A., Martin-Rodriguez, P., Lorenzo-Castrillejo, I., Ravelo, A.G., Fernandez-Perez, L., Machin, F. & Estevez-Braun, A. (2013) Synthesis and study of antiproliferative, antitopoisomerase II, DNA-intercalating and DNA-damaging activities of aryl-naphthalimides. *Bioorg. Med. Chem.*, **21**, 6484-6495.
- Ren, T., Xue, X., Wang, X., Zhou, X. & Dang, S. (2021) Bioinformatic and experimental analyses of key biomarkers in pancreatic cancer. *Exp. Ther. Med.*, **22**, 1359.
- Sampat, K., Kantarjian, H. & Borthakur, G. (2009) Clofarabine: emerging role in leukemias. *Expert Opin. Investig. Drugs*, **18**, 1559-1564.
- Siegel, R.L., Miller, K.D. & Jemal, A. (2017) Cancer statistics, 2017. *CA Cancer J. Clin.*, **67**, 7-30.
- Straus, D.J. (2003) Gallium nitrate in the treatment of lymphoma.

- Semin. Oncol.*, **30**, 25-33.
- Szklarczyk, D., Gable, A.L., Nastou, K.C., Lyon, D., Kirsch, R., Pyysalo, S., Doncheva, N.T., Legeay, M., Fang, T., Bork, P., Jensen, L.J. & von Mering, C. (2021) The STRING database in 2021: customizable protein-protein networks, and functional characterization of user-uploaded gene/measurement sets. *Nucleic Acids Res.*, **49**, D605-D612.
- Takahashi, T., Kanazawa, J., Akinaga, S., Tamaoki, T. & Okabe, M. (1999) Antitumor activity of 2-chloro-9-(2-deoxy-2-fluoro-beta-D-arabinofuranosyl) adenine, a novel deoxy-adenosine analog, against human colon tumor xenografts by oral administration. *Cancer Chemother. Pharmacol.*, **43**, 233-240.
- Tan, S., Sun, D., Lyu, J., Sun, X., Wu, F., Li, Q., Yang, Y., Liu, J., Wang, X., Chen, Z., Li, H., Qian, X. & Xu, Y. (2015) Antiproliferative and apoptosis-inducing activities of novel naphthalimide-cyclam conjugates through dual topoisomerase (topo) I/II inhibition. *Bioorg. Med. Chem.*, **23**, 5672-5680.
- Tan, S., Yin, H., Chen, Z., Qian, X. & Xu, Y. (2013) Oxo-heterocyclic fused naphthalimides as antitumor agents: synthesis and biological evaluation. *Eur. J. Med. Chem.*, **62**, 130-138.
- Tang, Z., Kang, B., Li, C., Chen, T. & Zhang, Z. (2019) GEPIA2: an enhanced web server for large-scale expression profiling and interactive analysis. *Nucleic Acids Res.*, **47**, W556-W560.
- Terashima, M., Ichikawa, W., Ochiai, A., Kitada, K., Kurahashi, I., Sakuramoto, S., Katai, H., Sano, T., Imamura, H. & Sasako, M.; ACTS-GC Group (2017) TOP2A, GGH, and PECAM1 are associated with hematogenous, lymph node, and peritoneal recurrence in stage II/III gastric cancer patients enrolled in the ACTS-GC study. *Oncotarget*, **8**, 57574-57582.
- Van Quaquebeke, E., Mahieu, T., Dumont, P., Dewelle, J., Ribaucour, F., Simon, G., Sauvage, S., Gaussin, J.F., Tuti, J., El Yazidi, M., Van Vynckt, F., Mijatovic, T., Lefranc, F., Darro, F. & Kiss, R. (2007) 2,2,2-Trichloro-N-({2-[2-(dimethylamino)ethyl]-1,3-dioxo-2,3-dihydro-1H-benzo[de] isoquinolin-5-yl} carbamoyl)acetamide (UNBS3157), a novel nonhematotoxic naphthalimide derivative with potent antitumor activity. *J. Med. Chem.*, **50**, 4122-4134.
- Wang, A., Chen, M., Wang, H., Huang, J., Bao, Y., Gan, X., Liu, B., Lu, X. & Wang, L. (2019) Cell adhesion-related molecules play a key role in renal cancer progression by multinet network analysis. *Biomed. Res. Int.*, **2019**, 2325765.
- Wang, Y., Zheng, B., Xu, M., Cai, S., Younseo, J., Zhang, C. & Jiang, B. (2020) Prediction and analysis of hub genes in renal cell carcinoma based on CFS gene selection method combined with adaboost algorithm. *Med. Chem.*, **16**, 654-663.
- Xu, D., Xu, Y., Lv, Y., Wu, F., Liu, Y., Zhu, M., Chen, D. & Bai, B. (2020) Identification of four pathological stage-relevant genes in association with progression and prognosis in clear cell renal cell carcinoma by integrated bioinformatics analysis. *Biomed. Res. Int.*, **2020**, 2137319.
- Ye, M., He, Z., Dai, W., Li, Z., Chen, X. & Liu, J. (2018) A TOP2A-derived cancer panel drives cancer progression in papillary renal cell carcinoma. *Oncol. Lett.*, **16**, 4169-4178.
- Yi, Y., Liu, Y., Wu, W., Wu, K. & Zhang, W. (2019) Reconstruction and analysis of circRNAmiRNAmRNA network in the pathology of cervical cancer. *Oncol. Rep.*, **41**, 2209-2225.
- Yuan, L., Zeng, G., Chen, L., Wang, G., Wang, X., Cao, X., Lu, M., Liu, X., Qian, G., Xiao, Y. & Wang, X. (2018) Identification of key genes and pathways in human clear cell renal cell carcinoma (ccRCC) by co-expression analysis. *Int. J. Biol. Sci.*, **14**, 266-279.
- Zhang, H., Zou, J., Yin, Y., Zhang, B., Hu, Y., Wang, J. & Mu, H. (2019) Bioinformatic analysis identifies potentially key differentially expressed genes in oncogenesis and progression of clear cell renal cell carcinoma. *PeerJ*, **7**, e8096.
- Zhang, X., Wang, Z., Zeng, Z., Shen, N., Wang, B., Zhang, Y., Shen, H., Lu, W., Wei, R., Ma, W. & Wang, C. (2021) Bioinformatic analysis identifying FGF1 gene as a new prognostic indicator in clear cell Renal Cell Carcinoma. *Cancer Cell Int.*, **21**, 222.
- Zhenchuk, A., Lotfi, K., Juliusson, G. & Albertioni, F. (2009) Mechanisms of anti-cancer action and pharmacology of clofarabine. *Biochem. Pharmacol.*, **78**, 1351-1359.
- Zhou, W.M., Wu, G.L., Huang, J., Li, J.G., Hao, C., He, Q.M., Chen, X.D., Wang, G.X. & Tu, X.H. (2019) Low expression of PDK1 inhibits renal cell carcinoma cell proliferation, migration, invasion and epithelial mesenchymal transition through inhibition of the PI3K-PDK1-Akt pathway. *Cell. Signal.*, **56**, 1-14.
- Zou, Y., Zhou, J., Xu, B., Li, W. & Wang, Z. (2019) Ribonucleotide reductase subunit M2 as a novel target for clear-cell renal cell carcinoma. *Onco Targets Ther.*, **12**, 3267-3275.